A New Single-Stage Three-Phase PFC for Four-Switch Three-Phase Inverter Fed IM Drives

Mohamed ZAKY[1,3*], Tamer FETOUH[1,3], Haitham AZAZI[2,3]
[1]*Department of Electrical Engineering, Northern Border University, Arar, 1321, Saudi Arabia*
[2]*Department of Electrical Engineering, Minoufiya University, Shebin El-Kom, 32511, Egypt*
[3]*Department of Electrical Engineering, College of Engineering, King Khalid University, Abha 61421, Saudi Arabia*
[*]*mszaky78@yahoo.com*

***Abstract*—This paper proposes a single-stage three-phase power factor correction (PFC) for four-switch inverter (FSI) fed induction motor (IM) drives. The PFC scheme uses a Cuk converter with only one switch, and consequently, it needs only one control signal. This attains low computation burden, simple control algorithm, and minimum cost. A new PFC control technique is proposed to guarantee sinusoidal supply currents with high power factor (PF) and low total harmonic distortion (THD). Moreover, the PFC technique regulates the DC bus voltage. Equivalent circuits of the Cuk converter operating in two modes are deduced, its mathematical modeling and analysis are performed. The proposed drive system is built using MATLAB/Simulink and operates in real-time using a prototype system which consists of a DSP-DS1104 digital control board and an IM. The efficacy of the Cuk converter is verified by extensive tests in various operating conditions.**

***Index Terms*—induction motors, inverters, converters, motor drives, machine vector control.**

I. INTRODUCTION

The use of induction motor (IM) drives in the industry has increased in practical applications. Inverters are considered an important part in the IM drive system [1]. Conventional IM drives have three-phase converters with a capacitor filter to transform a DC rectified voltage to an AC voltage with variable magnitude and frequency [2]. The inverters require 3-phase uncontrolled diode bridge rectifiers [3]. Capacitors were utilized to smooth the DC output rectified voltage. AC/DC rectifier circuits produce unregulated current signal with non-sinusoidal shape [4]. Different complex issues related to the resultant harmonics and losses were created. These issues reflect on the AC source and reduce the power source quality [5]. The most undesired issues are injecting current harmonics in the grid, overheating the instruments, voltage distortion at the point of common coupling, reduced power factor (PF), and minimized efficiency [6]-[7]. International standards indicate the limits of different harmonics of the current and voltage waves [8]-[9]. The current should be reconstructed to be a sine wave [10]-[11], what improve the PF and minimize the losses [12]. So new power factor correction (PFC) topologies for AC-DC converters were necessary to mitigate the power source quality issues [13]-[14]. These topologies use numerous switches and complex control circuits and have increased costs [15].

Different PFC schemes for DC-DC converters are employed [16-17]. The main common scheme is the boost converter; however, it has a shortcoming. The value of output voltage exceeds the peak supply voltage. Therefore, the output cannot be simply isolated from the input. Cuk and Flyback were employed in applications which need step-down/step-up transformation. Accordingly, Flyback scheme treats the previous drawback [18]. In this paper, the Cuk scheme for PFC was utilized. This scheme presents isolated output-input with limited inrush current at starting. Also, it has the capability of step-up/down output voltage [19-20].

Nowadays, the tendency is to develop compact and cheap IM drives. Traditional six-switch inverters (SSI) were commonly employed for variable-speed drives (VSDs). Therefore, great exertions were done to replace SSI with four-switch inverter (FSI) for uninterruptible power supply and VSDs [21-24]. Several features are realized with replacing traditional SSI with FSI in terms of reliability, simplicity, low computation burden, and low price [25]-[28].

This paper proposes the following new contributions:

1) Designs a single-stage three-phase PFC of FSI fed IM drive using a Cuk converter with only one switch.
2) Proposes a new technique to control the input PF with a minimized total harmonic distortion (THD) and to regulate the output voltage of the Cuk converter. The control structure is simple and has a small cost.
3) Presents the influences of the suggested PFC topology on the power source quality issues.
4) Executes the drive system with the proposed PFC technique in Matlab/Simulink, and in the laboratory.
5) Provides extensive tests under various working conditions to validate the usefulness of the suggested control.

Compared to the previous state-of-the-art works, the solution proposed by this paper offers the following advantages:

1) A simple control circuit,
2) Low cost of the drive system, and
3) Low computation burden.

II. PROPOSED SYSTEM STRUCTURE

The proposed PFC circuit is presented in Fig. 1. The system consists of the power circuit and two major control circuits. The power circuit composes of three-phase power supply

The authors gratefully acknowledge the approval and the support of this research study by the grant no. ENG-2017-1-8-F-7230 from the Deanship of Scientific Research at Northern Border University, Arar, KSA.

Digital Object Identifier 10.4316/AECE.2019.02011

which feeds three-phase full wave rectifier. The output of rectifier circuit is the input of the DC-DC Cuk converter which is used for PFC of the power supply. The Cuk converter contains of three inductors (L_{sa}, $L_{sb,}$ *and* L_{sc}), the capacitor (C), the diode (D), the inductor (L) and a single switch (S). The three inductors (L_{sa}, $L_{sb,}$ *and* L_{sc}) are located between the input power supply and rectifier. Since the Cuk converter contains a single power switch, the control circuit has a simple structure; built with analog circuits or a low-cost microprocessor. The regulated DC voltage of Cuk converter is the input to FSI (T_1, T_2, $T_{3,}$ and T_4) which feeds the three-phase squirrel cage IM. The drive system consists of two main control schemes; PFC control to develop a high PF for the input supply and field oriented control (FOC) to control the speed of a three-phase IM.

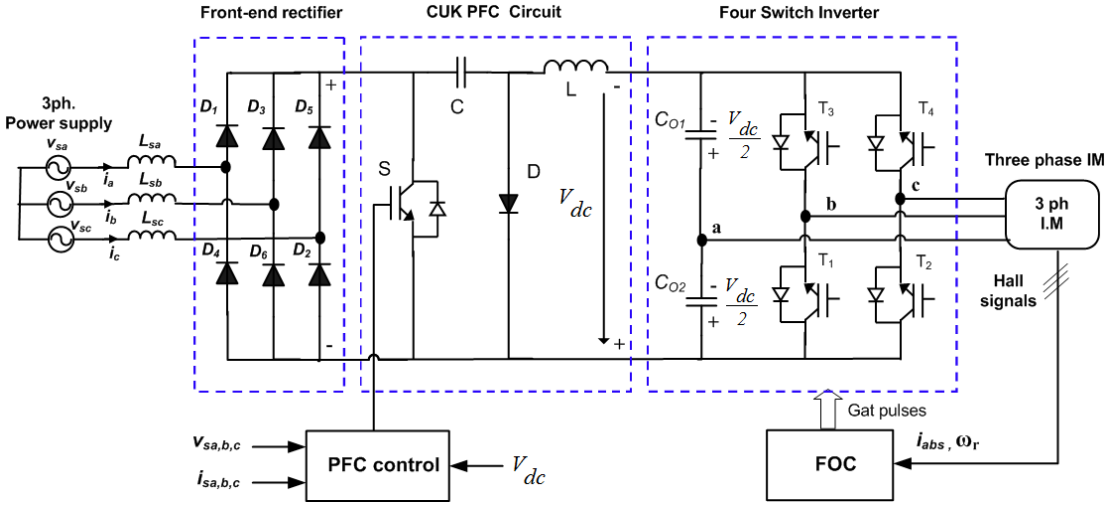

Figure 1. Proposed PFC for three–phase AC-DC Cuk fed FSI of IM

III. CUK CONVERTER ANALYSIS

The Cuk converter works in a continuous conduction mode (CCM) and has two operation modes with the help of three-phase input voltage waveforms of Fig. 2.

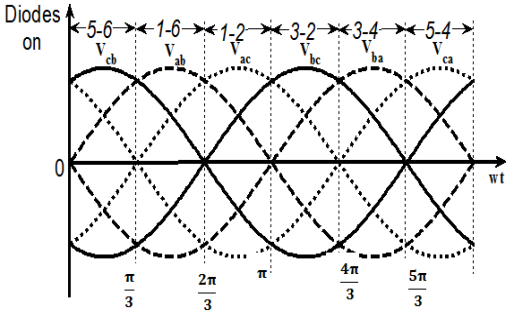

Figure 2. waveforms of input voltages

A. *Mode 1 of Operation*

The switch *S* is on in this operation mode as shown in Fig. 3. Therefore, the input currents (i_a, i_b, *and* i_c) increase and the inductors (L_{sa}, $L_{sb,}$ *and* L_{sc}) store the energy. The capacitor (C) discharges and transmits its energy to the output capacitors (C_{o1} and C_{o2}).

The three-line supply voltages (v_{sab}, v_{sbc}, and v_{sca}) can be written as:

$$\begin{cases} v_{sab} = V_{lm}\sin(\omega_s t) \\ v_{sbc} = V_{lm}\sin(\omega_s t - 2\pi/3) \\ v_{sca} = V_{lm}\sin(\omega_s t + 2\pi/3) \end{cases} \quad (1)$$

where, V_{lm} is the maximum line voltage and ω_s is the supply frequency.

The line voltage equations of the Cuk converter can be written as follow:

$$v_{scb} = L_{sc}\frac{di_c}{dt} - L_{sb}\frac{di_b}{dt} \qquad \text{for } \theta = 0 \to \frac{\pi}{3} \qquad (2)$$

$$v_{sab} = L_{sa}\frac{di_a}{dt} - L_{sb}\frac{di_b}{dt} \qquad \text{for } \theta = \frac{\pi}{3} \to \frac{2\pi}{3} \qquad (3)$$

$$v_{sac} = L_{sa}\frac{di_a}{dt} - L_{sc}\frac{di_c}{dt} \qquad \text{for } \theta = \frac{2\pi}{3} \to \pi \qquad (4)$$

$$v_{sbc} = L_{sb}\frac{di_b}{dt} - L_{sc}\frac{di_c}{dt} \qquad \text{for } \theta = \pi \to \frac{4\pi}{3} \qquad (5)$$

$$v_{sba} = L_{sb}\frac{di_b}{dt} - L_{sa}\frac{di_a}{dt} \qquad \text{for } \theta = \frac{4\pi}{3} \to \frac{5\pi}{3} \qquad (6)$$

$$v_{sca} = L_{sc}\frac{di_c}{dt} - L_{sa}\frac{di_a}{dt} \qquad \text{for } \theta = \frac{5\pi}{3} \to 2\pi \qquad (7)$$

B. *Mode 2 of Operation*

The switch *S* is off in this mode as shown in Fig. 4. Therefore, the input currents decrease and the inductors (L_{sa}, $L_{sb,}$ *and* L_{sc}) convert their stored energy to the capacitor (C). Also, the stored energy in the inductor (L) transmits to the output capacitors (C_{o1} and C_{o2}).

The line voltage equations are derived as follow:

$$v_{scb} = L_{sc}\frac{di_c}{dt} + \frac{1}{C}\int i_c dt + v_{co} - L_{sb}\frac{di_b}{dt} \qquad \text{for } \theta = 0 \to \frac{\pi}{3} \quad (8)$$

$$v_{sab} = L_{sa}\frac{di_a}{dt} + \frac{1}{C}\int i_a dt + v_{co} - L_{sb}\frac{di_b}{dt} \qquad \text{for } \theta = \frac{\pi}{3} \to \frac{2\pi}{3} \quad (9)$$

$$v_{sac} = L_{sa}\frac{di_a}{dt} + \frac{1}{C}\int i_a dt + v_{co} - L_{sc}\frac{di_c}{dt} \qquad \text{for } \theta = \frac{2\pi}{3} \to \pi \quad (10)$$

$$v_{sbc} = L_{sb}\frac{di_b}{dt} + \frac{1}{C}\int i_b dt + v_{co} - L_{sc}\frac{di_c}{dt} \qquad \text{for } \theta = \pi \to \frac{4\pi}{3} \quad (11)$$

$$v_{sba} = L_{sb}\frac{di_b}{dt} + \frac{1}{C}\int i_b dt + v_{co} - L_{sa}\frac{di_a}{dt} \qquad \text{for } \theta = \frac{4\pi}{3} \to \frac{5\pi}{3} \quad (12)$$

$$v_{sca} = L_{sc}\frac{di_c}{dt} + \frac{1}{C}\int i_c dt + v_{co} - L_{sa}\frac{di_a}{dt} \qquad \text{for } \theta = \frac{5\pi}{3} \to 2\pi \quad (13)$$

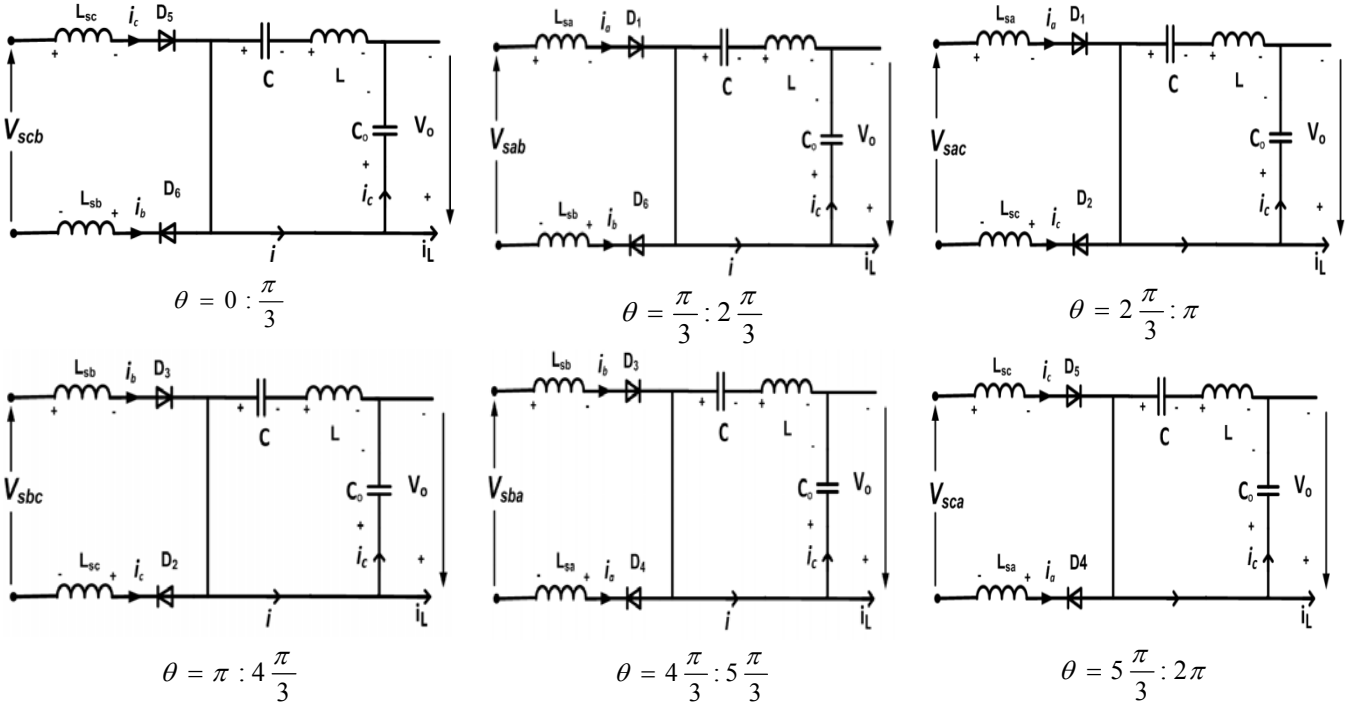

Figure 3. Equivalent circuit of Cuk converter for mode 1

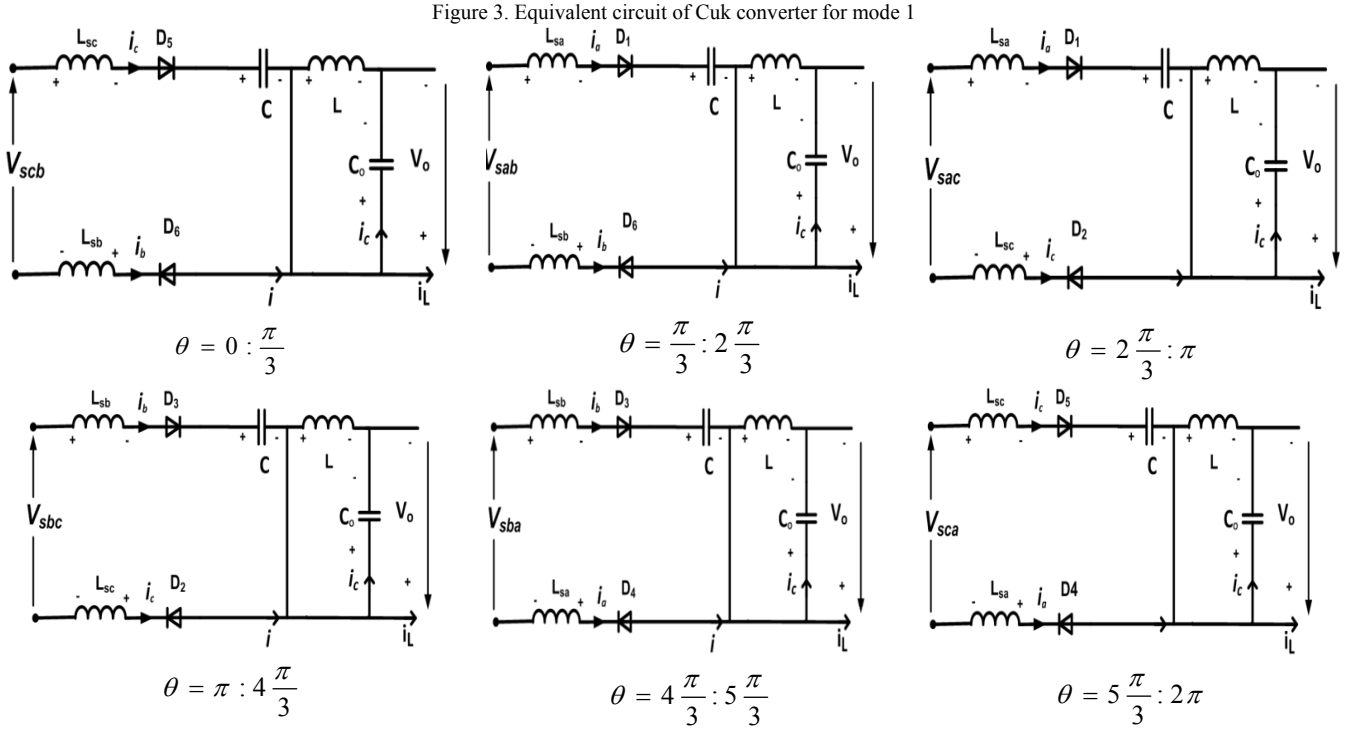

Figure 4. Equivalent circuit of Cuk converter for mode 2

IV. PROPOSED PFC METHOD

Fig. 5 presents the proposed Cuk PFC scheme. The PFC control gives sinusoidal supply current waveforms with low THD, high PF, and smooth DC bus voltage.

The next steps are followed to design the PFC control method.

a) The three-phase input voltages (v_{sa}, v_{sb}, and v_{sc}) are measured to get the unit signals of input voltages ($|v_{sa}|$, $|v_{sb}|$, and $|v_{sc}|$).

b) The proportional integral (PI) voltage controller is used to regulate the DC link voltage and can be expressed by

$$I_{VR} = (K_P + K_I \int dt)(v_{ref} - v_{dc}) \tag{14}$$

where, the voltage reference (v_{ref}) depends on the desired output voltage, K_P and K_I are the proportional and integral gains of PI controller, I_{VR} is the output of the DC bus voltage controller.

c) The supply current references (i_a^*, i_b^*, and i_c^*) can be calculated by multiplying I_{VR} with the unit signals of input voltages as follow:

$$i_a^* = |v_{sa}| \times I_{VR} \tag{15}$$

$$i_b^* = |v_{sb}| \times I_{VR} \tag{16}$$

$$i_c^* = |v_{sc}| \times I_{VR} \tag{17}$$

where,

$$|v_{sa}| = |\sin(\omega_s t)| \tag{18}$$

$$|v_{sb}| = |\sin(\omega_s t - 2\pi/3)| \quad (19)$$

$$|v_{sc}| = |\sin(\omega_s t + 2\pi/3)| \quad (20)$$

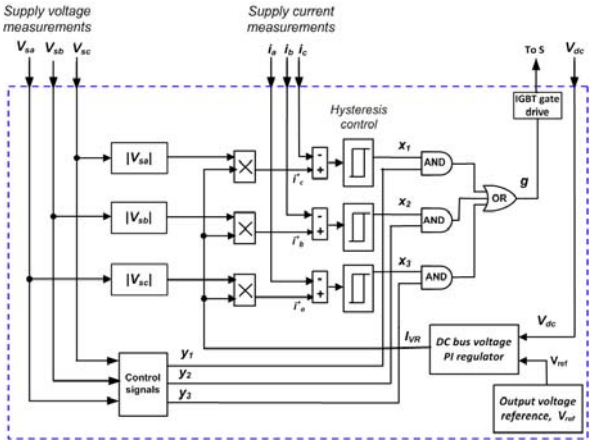

Figure 5. Proposed Cuk PFC control.

d) Three hysteresis current regulators are used to force the three-phase supply currents (i_a, i_b, and i_c) to follow their corresponding reference currents which are in phase with supply voltages to obtain the unity PF. The outputs of these regulators are the signals x_1, x_2, and x_3

e) The control signals block is designed to specify the higher value of the three-phase input voltages for each period. It consists of two stages. The first stage has six relational operators which compare each phase voltage with the other two phases to specify the larger one as shown in Fig. 6a. The second stage has three AND gates; built with two inputs as shown in Fig. 6b. The outputs of this stage are the signals y_1, y_2 and y_3.

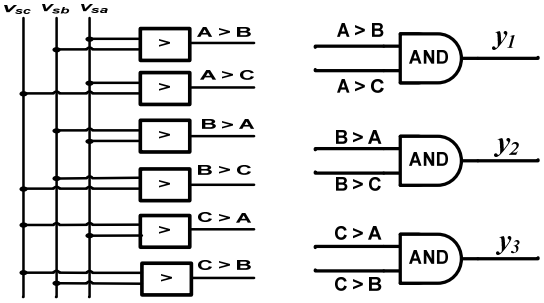

(a) (b)

Figure 6. Control signals block: (a) First stage of the logic circuit and (a) Second stage of the logic circuit.

f) The logic AND gates are used to compare the signals x_1, x_2, and x_3 with the signals y_1, y_2, and y_3.

g) The switch gate signal (g) is obtained from the outputs of the current controllers and the three control signals using (21).

$$g = x_1 \times y_1 + x_2 \times y_2 + x_3 \times y_3 \quad (21)$$

h) The PF depends on the THD of supply current and K_θ as shown in the following equation:

$$PF = \frac{1}{\sqrt{1+(\frac{THD}{100})^2}} K_\theta \quad (22)$$

where, K_θ is the displacement angle between the supply voltage and current.

V. Model And The Control Of IM

A. Model of IM

The motor stator voltages in d-q stationary reference frame (v_{qs}^s and v_{ds}^s) can be given by,

$$v_{qs}^s = \sqrt{2/3}(v_a - 0.5(v_b + v_c)) \quad (23)$$

$$v_{ds}^s = \sqrt{2/3}(-(\sqrt{3}/2)v_b + (\sqrt{3}/2)v_c) \quad (24)$$

Where, v_a , v_b, and v_c are the three-phase stator voltages.

The differential equations of three-phase IM in stationary reference frame are expressed in a matrix form by:

$$\begin{bmatrix} v_{qs}^s \\ v_{ds}^s \\ 0 \\ 0 \end{bmatrix} = \begin{bmatrix} r_s & 0 & 0 & 0 \\ 0 & r_s & 0 & 0 \\ 0 & 0 & r_r & 0 \\ 0 & 0 & 0 & r_r \end{bmatrix} \begin{bmatrix} i_{qs}^s \\ i_{ds}^s \\ i_{qr}^s \\ i_{dr}^s \end{bmatrix} + \begin{bmatrix} \dot{\lambda}_{qs}^s \\ \dot{\lambda}_{ds}^s \\ \dot{\lambda}_{qr}^s \\ \dot{\lambda}_{dr}^s \end{bmatrix} + \begin{bmatrix} 0 \\ 0 \\ -\omega_r \lambda_{dr}^s \\ \omega_r \lambda_{qr}^s \end{bmatrix} \quad (25)$$

where:

$$\begin{bmatrix} \lambda_{qs}^s \\ \lambda_{ds}^s \\ \lambda_{qr}^s \\ \lambda_{dr}^s \end{bmatrix} = \begin{bmatrix} L_s & 0 & L_m & 0 \\ 0 & L_s & 0 & L_m \\ L_m & 0 & L_r & 0 \\ 0 & L_m & 0 & L_r \end{bmatrix} \begin{bmatrix} i_{qs}^s \\ i_{ds}^s \\ i_{qr}^s \\ i_{dr}^s \end{bmatrix} \quad (26)$$

The electromagnetic torque is given by,

$$T_e = \frac{3}{4}(\frac{p}{2})(i_{qs}^s i_{dr}^s - i_{ds}^s i_{qr}^s) \quad (27)$$

The motor speed in rad/sec is given by,

$$\dot{\omega}_r = (T_e - T_l - F\omega_r)/J \quad (28)$$

where,

v_{ds}^s and v_{qs}^s are dq stator voltages,

i_{ds}^s and i_{qs}^s are dq stator currents,

i_{dr}^s and i_{qr}^s are dq rotor currents,

λ_{ds}^s and λ_{qs}^s are dq stator flux linkages,

λ_{dr}^s and λ_{qr}^s are dq rotor flux linkages,

r_s and r_r are the stator and rotor resistances of IM,

L_m, L_s, *and* L_r are magnetizing inductance, stator inductance, and rotor inductance, respectively, ω_r is the electrical rotor speed, p is the number of poles, J is the motor inertia, F is the viscous friction, T_e and T_l are the motor and load torques.

The no-load and short-circuit tests are used to obtain the IM parameters as given in Table I in the appendix.

B. FOC of the IM

Fig. 7 shows the FOC of three-phase IM. The difference between the motor speed ω_r and the reference speed ω_{ref} is passed through PI speed controller to give the reference torque T_e^*. The quadrature and direct reference currents (i_{sq}^* and i_{sd}^*) are calculated using (29).

$$i_{sq}^{e*} = (\frac{4}{3p})(\frac{L_r T_e^*}{L_m \lambda_r^*}) \quad (29)$$

$$i_{sd}^{e*} = \left(\frac{\lambda_r^*}{L_m}\right) \tag{30}$$

Theses currents are transformed to the reference motor currents (i_a^* , i_b^* , and i_c^*). The hysteresis current controller is used to compare the measured motor currents with their corresponding reference currents to produce the gate pulses as shown in Fig. 7.

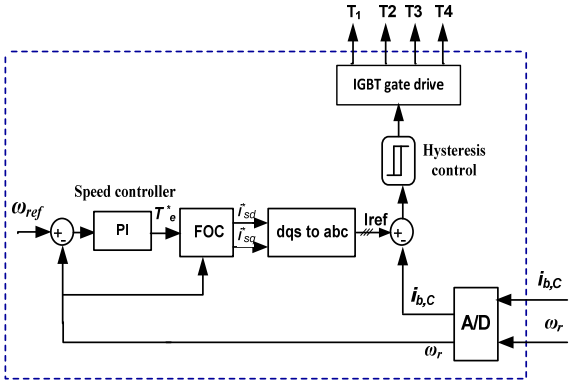

Figure 7. FOC of a three-phase IM

C. Selection of the PI Controller Gains

The speed controller is of utmost importance for the industrial applications. Different nonlinear and linear controllers for various applications are recently presented [29]-[30]

Actually, the PI controller gains affect the speed response in terms of the settling time, rising time, overshoot and undershoot values, and load torque rejection. Therefore, they need to be adjusted to provide a good response.

The simplified block diagram of the speed control of IM drive is presented in Fig. 8. The open-loop transfer function of the drive system is described using Eqn. (31). It has one zero at $-K_{i\omega}/K_{p\omega}$, and two poles at zero and $-F/J$.

$$G_{OL}\big|_{T_L=0} = \frac{K_p K_t \left(s + K_{i\omega}/K_{p\omega}\right)}{(Js+F)s} \tag{31}$$

The PI controller gains are selected using Root-locus plot as shown in Fig. 9. It is found that the PI gains ($K_{i\omega} = 6$ and $K_{p\omega} = 1$) are selected to give the best dynamic response.

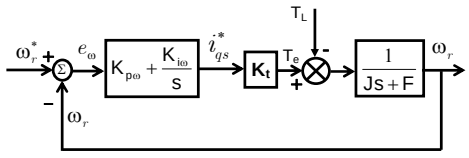

Figure. 8 Simplified block diagram for the speed controller of the IM drive

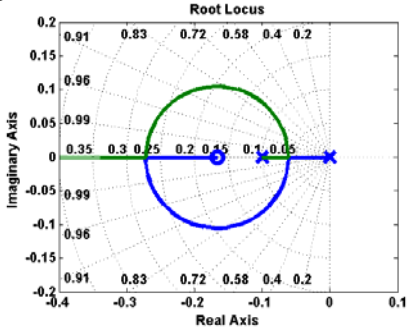

Figure. 9 Root locus plot the open-loop transfer function with the PI controller gains $K_{p\omega} = 1$ and $K_{i\omega} = 6$

VI. Results and Discussion

A. Experimental Setup

The proposed PFC circuit can be built using MATLAB/Simulink as shown in Fig. 10. The simulation program is saved in a webpage link as cited in the appendix for validation purposes. The parameter values are listed in Table II in the Appendix. The experimental system was implemented in the laboratory to prove the system performance. The supply phase voltage and reference DC link voltage are set at 220 V (rms) and 1000 V, respectively. Fig. 11 shows the schematic diagram of the experimental layout. It consists of power and control circuits. The controller is carried out in real time by DS1104 control board. The power circuit consists of three-phase AC supply with a grid line voltage of 380 V, three inductors, three-phase rectifier, DC-DC Cuk converter, FSI, and IM. A separately excited DC generator is coupled with the IM for loading tests. Cuk converter consists of a switch, capacitors, a fast recovery diode (type DESI 60) and a coil. The power switches used in the converter and inverter circuits are IGBT type (CM100DY-24H). The motor speed is measured using incremental shaft encoder type (RI 58). Voltage sensors (LV25-P) and current sensors (LA25-NP) were used for the required voltage and current measurements.

B. Design Process of the Drive System

The next design steps are followed to build the drive system (PFC control and FOC):

1) Sets the parameters in the memory, gets the references voltage and speed, and starts timers.
2) Sends the measurement signals to the DSP using dSPACE -DS1104 control board via the A/D converter ports.
3) Increases the input voltages to a line voltage of 380 V using the autotransformer.
4) Builds the model of the Cuk PFC control scheme using the power system block set tool in the MATLAB/Simulink.
5) Calculates the gate pulse of the Cuk converter for PFC and DC voltage regulation using Eqs. (14)-(21).
6) Builds the simulation model of FOC strategy using Eqs. (23)-(28).
7) The actual supply currents can be controlled to follow the corresponding references of supply current using three hysteresis current regulators as shown in Fig. 5.
8) The dSPACE board has facilitated to capture the experimental waveforms and to export them numerically per sample.

The ratings of the experimental circuit are found in Appendix.

B. Simulation and Experimental Results

Fig. 12 shows simulation and experimental tests for Cuk PFC fed FSI three-phase IM at full-load torque (7 N.m) and reference speed of 120 rad/sec. This figure presents the phase supply voltage and current. As seen, the supply current is in phase with its voltage and nearly sinusoidal. Three-phase supply currents are shown in Fig. 13. As observed, the supply currents are nearly sinusoidal and

symmetrical. The supply current harmonics are compared with the standard IEC 61000-3-2 class A limits as shown in Fig. 14. The supply current has a THD of 2.55% and 4.5% and a PF of 0.9997 and 0.99797 for simulation and experimental, respectively. DC bus voltage, motor speed, and motor currents are shown in Figs. 15 and 16, respectively. It is clear that the bus voltage and motor speed are kept at its reference value.

The experimental system is tested under a step change in load toque (from 2 to 7 N.m) at motor speed of 120 rad/sec and reference output voltage of 1000 V as shown in Fig. 17. It is indicated that the DC bus voltage remained constant at its reference. The robustness of the proposed system is checked also at a step change in the reference motor speed from 100 to 120 rad/sec as illustrated in Fig. 18. As noted, the DC bus voltage achieves a fast recovery time to its reference value.

Table III shows a comparison with previous works [13], [31]-[32]. The proposed PFC technique proves cost effective because it has minimum components. Moreover, it has lower PF and THD than the previous works.

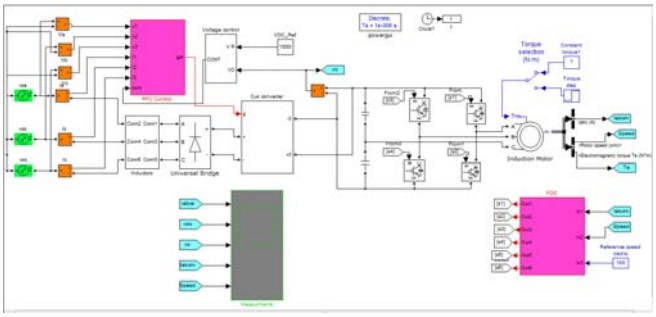

Figure. 10 Simulation model of the drive system using MATLAB/Simulink program.

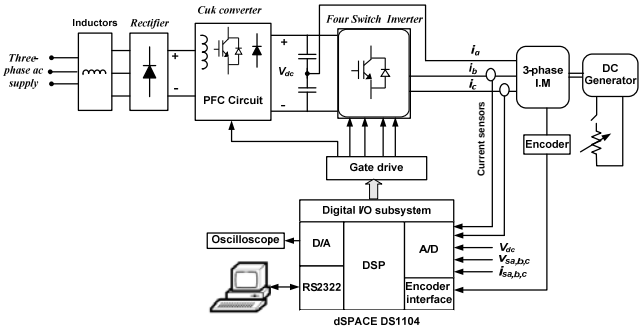

Figure 11. Experimental system block diagram

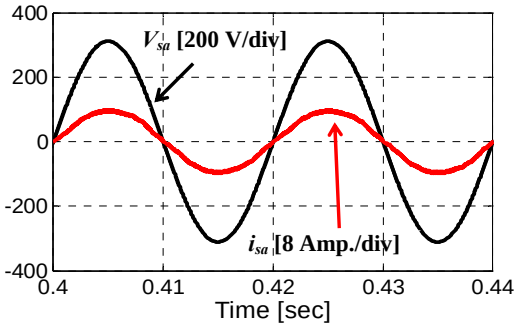

(a) Simulation

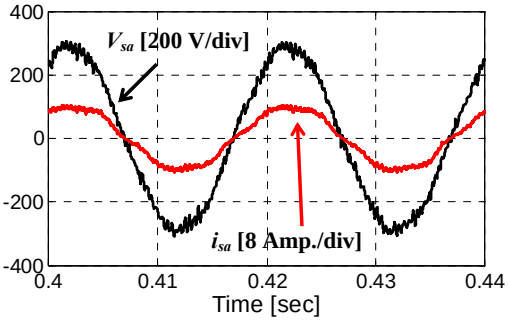

(b) Experimental

Figure 12. Simulation and experimental tests showing steady state performance of supply phase voltage and current.

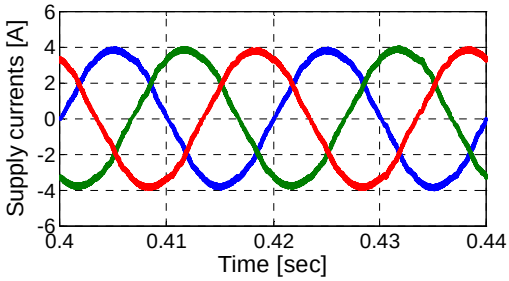

(a) Simulation

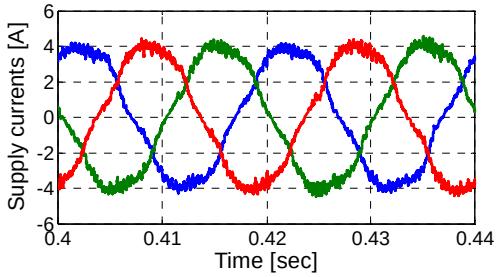

(b) Experimental

Figure 13. Simulation and experimental tests showing steady state performance of supply currents.

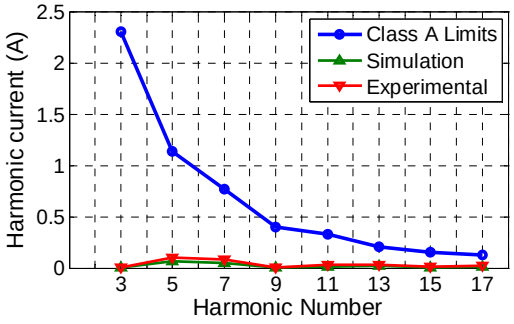

Figure 14. Simulation and experimental tests showing steady state performance of supply current harmonics.

TABLE III. COMPARISON WITH PREVIOUS WORKS

Method / Items	Two modules boost PFC [13]	Isolated SEPIC PFC [31]	Three modules Cuk converter [32]	Propose PFC Technique
Components count	2-IGBTs + 2-Diodes	3-IGBTs + 3-Diodes	3-IGBTs + 3-Diodes	1-IGBTs + 1-Diodes
Passive elements	2-L + 2-C	3-L + 3-C	7-L + 10-C	4-L + 2-C
Additional elements	2-Tranformer+2-Rectifier	3-Tranformer+3-Rectifier	3-Tranformer+3-Rectifier	1-Rectifier
No. of controller	2	1	1	1
THD %	3.6	4.03	2.68	2.55
Power factor	0.995	0.9987	0.9996	0.9997

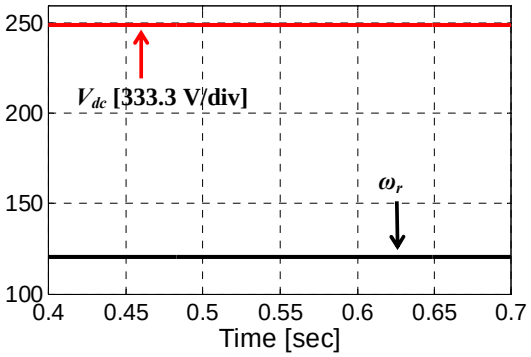

(a) Simulation

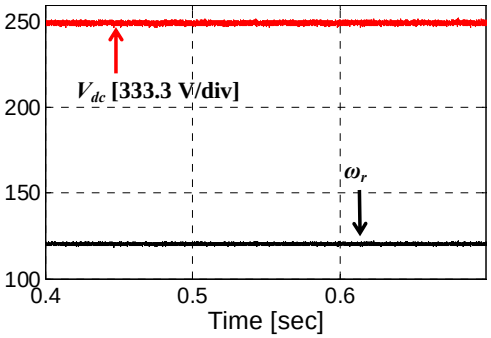

(b) Experimental

Figure 15. Simulation and experimental tests showing steady state performance of DC bus voltage and motor speed.

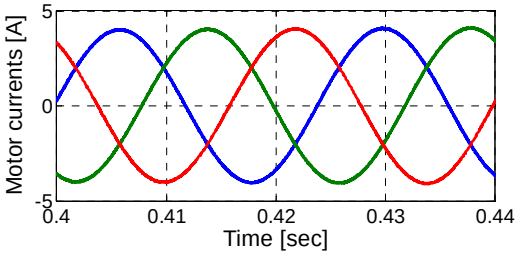

(a) Simulation

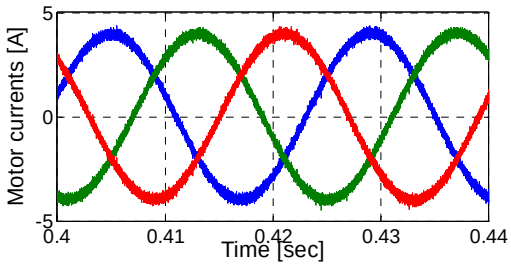

(b) Experimental

Figure 16. Simulation and experimental tests showing steady state performance of motor currents

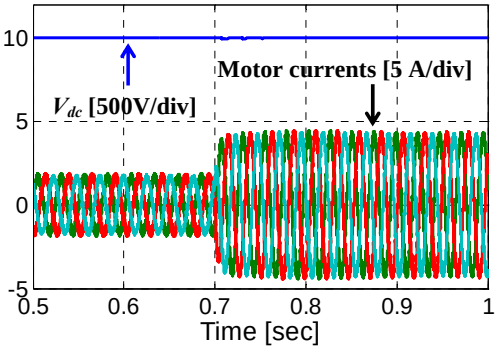

(a) Simulation

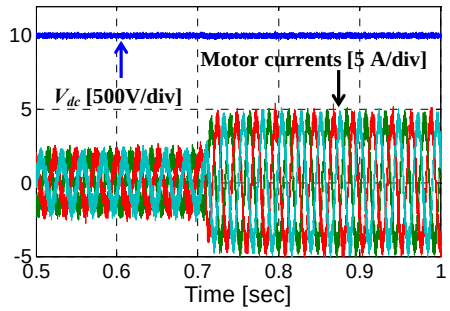

(b) Experimental

Figure 17. Simulation and experimental tests showing transient performance for step load toque variation

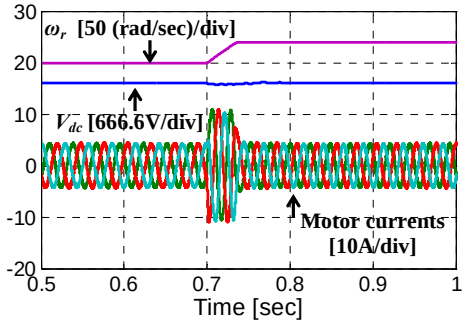

(a) Simulation

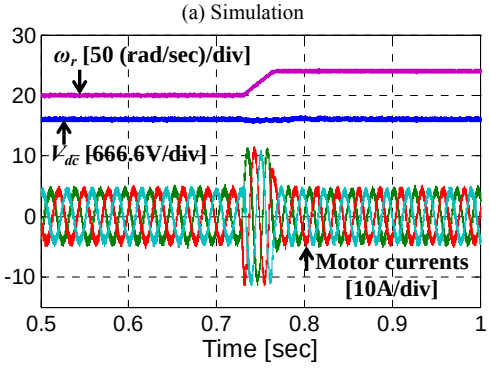

(b) Experimental

Figure 18. Simulation and experimental tests showing transient performance for step variation in motor speed

VII. Conclusion

In this paper, a new single-stage three-phase PFC of FSI fed IM drive is proposed. The proposed Cuk converter uses one switch with simple control circuit and low cost. The FSI was used to feed IM drive and developed on the same DSP card with PFC control for cost reduction. Influences of the proposed PFC topology on the power source quality issues have been presented. The AC drive system with the proposed converter control has been executed in both Matlab/Simulink program, and also in the laboratory. Extensive tests under various working conditions were captured to validate the usefulness of the proposed control. The proposed system has the following advantages: simple control structure, minimum THD in the supply current, high input PF, good regulated dc bus voltage, and simple implementation of the control circuit.

Appendix

TABLE I. Specifications of IM

Motor Rating	1.5 Hp	L_S	0.0221 H
Voltage	380 V	L_r	0.0221 H
Frequency	50 Hz	L_m	0.4114 H
No. of poles (2*p*)	4	J	0.02 kg.m^2
r_S	7.4826 ohm	Connection	star
r_r	3.6840 ohm	RPM	1420

TABLE II. CONVERTER PARAMETERS

Parameters	Values
$v_{sab} = v_{sbc} = v_{sca}$	380 V, rms
ω_s	314 rad/sec
$L_{sa=} L_{sb=} L_{sc}$	7 mH
C	20 μF
L	3 mH
$C_{o1}= C_{o2}$	1000 μF

LINK TO SIMULATION PROGRAMS

https://gulfupload.com/ecr2dnciwskc

REFERENCES

[1] J. W. Finch, D. Giaouris, "Controlled AC Electrical Drives," IEEE Trans. on Industrial Electronics, vol. 55, no. 2, pp. 481-491, 2008. doi:10.1109/TIE.2007.911209

[2] C. Jui-Y, L. Chang-Ming, "Development of a Switched-Reluctance Motor Drive with PFC Front End," IEEE Trans. on Energy Conversion, vol. 24, no. 1, pp. 30-42, 2009. doi:10.1109/TEC.2008.2002328

[3] I. Jun-ichi, O. Nobuhiro, "Square-Wave Operation for a Single-Phase-PFC Three-Phase Motor Drive System without a Reactor," IEEE Trans. on Industry Applications, vol. 47, no. 2, pp. 805-811, 2011. doi:10.1109/TIA.2010.2102736

[4] H. Z. Azazi, E. E. El-Kholy, S. A. Mahmoud, S. S. Shokralla, "Power Factor Correction using Predictive Current Control for Three Phase Induction Motor Drive System," Electric Power Components and Systems, vol. 42, no. 2, pp. 190-202, 2014. doi:10.1080/15325008.2013.853218

[5] B. Singh, B.N. Singh, A. Chandra, K. Al-Haddad, A. Pandey, D. P. Kothari, "A Review of Three-phase Improved Power Quality AC-DC Converters," IEEE Transactions on Industrial Electronics, vol. 51, no. 3, pp. 641-660, 2004. doi:10.1109/TIE.2004.825341

[6] J. O. Estima, A. J. M. Cardoso, "A New Algorithm for Real-Time Multiple Open-Circuit Fault Diagnosis IN Voltage-Fed PWM Motor Drives by the Reference Current Errors," IEEE Trans. on Industrial Electronics, vol. 60, no. 8, pp. 3496-3505, 2013. doi:10.1109/TIE.2012.2188877

[7] S. Bhim, G. Bhuvaneswari, V. Garg, "Power-Quality Improvements in Vector-Controlled Induction Motor Drive Employing Pulse Multiplication in AC-DC Converters." IEEE Transactions on Power Delivery, vol. 21, no. 3, pp. 1578-1586, 2006. doi:10.1109/TPWRD.2006.874660

[8] Compliance Testing to the IEC 1000-3-2 (EN 61000-3-2) and IEC 1000-3-3 (EN 61000- 2-3) Standards, Application Note 1273, Hewlett Packard Co., 1995.

[9] IEEE guide for harmonic control and reactive compensation of Static Power Converters, IEEE Standard 519-1992. doi:10.1109/IEEESTD.1981.81020

[10] G. Bhuvaneswari, B. Singh, S. Madishetti, "Three-Phase, Two-Switch PFC Rectifier Fed Three-Level VSI Based FOC of Induction Motor Drive" IEEE Fifth Power India Conference, 2012. doi:10.1109/PowerI.2012.6479577

[11] A. R. Al-Ali, M. M. Negm, M. Kassas, "A PLC based power factor controller for a 3-phase induction motor," IEEE Industry Applications Conference, 2000. doi:10.1109/IAS.2000.881964

[12] N. Zabihi, R. Gouws, "Improving Energy Consumption of an Induction Motor by Design of a Power Factor Correction System and Estimation of it's saving on a Large Scale," IEEE International Conference on Industrial and Commercial Use of Energy (ICUE), 2014. doi:10.1109/ICUE.2014.6904192

[13] G. Bhuvaneswari, Bhim Singh, S. Madishetti, "Three-Phase, Two-Switch PFC Rectifier Fed Three-Level VSI Based FOC of Induction Motor Drive," IEEE Fifth Power India Conference, 2012. doi:10.1109/PowerI.2012.6479577

[14] R. Krishnan, D. Diamantidis, S. Lee, "Impact of Power Factor Correction on Low Power Inverter-Fed Induction Motor Drive System," 26th Annual IEEE Power Electronics Specialists Conference, PESC'95, vol. 1, 1995. doi:10.1109/PESC.1995.474869

[15] M. Gonzalez-Ramirez, C. A. Cruz-Villar, "Variable Speed Drive with PFC Front-End for Three-Phase Induction Motor" IET Electronics Letters, vol. 53, no. 16, pp. 1139-1140, 2017. doi:10.1049/el.2017.1671

[16] U. Kamnarn, V. Chunkag, "Analysis and Design of a Modular Three-Phase AC-to-DC Converter Using CUK Rectifier Module With Nearly Unity Power Factor and Fast Dynamic Response," IEEE Transactions on Power Electronics, vol. 24, no. 8, pp. 2000–2012, 2009. doi:10.1109/TPEL.2009.2019575

[17] H. C. Chiang, F. J. Lin, J. K. Chang, K. F. Chen, Y. L. Chen, K. C. Liu, "Control Method for Improving the Response of Single-Phase Continuous Conduction Mode Boost Power Factor Correction Converter," IET Power Electronics, vol. 9, no. 9, pp. 1792-1800, 2016. doi:10.1049/iet-pel.2015.0914

[18] L. S. Yang, T. J. Liang, J. F. Chen, "Analysis and Design of a Novel Three-Phase AC–DC Buck-Boost Converter," IEEE Transactions on Power Electronics, vol. 23, no. 2, pp. 707 – 714, 2008. doi:10.1049/iet-pel:20070013

[19] M. G. Umamaheswari, G. Uma, K. M. Vijayalakshmi, "Analysis and Design of Reduced-Order Sliding-Mode Controller for Three-Phase Power Factor Correction Using Cuk Rectifiers," IET Power Electronics, vol. 6, no. 5, pp. 935-945, 2013. doi:10.1049/iet-pel.2012.0402

[20] S. Singh, B. Singh, "A Voltage-Controlled PFC Cuk Converter-Based PMBLDCM Drive for Air-Conditioners," IEEE Transactions on Industry Applications, vol. 48, no. 2, pp. 832-838, 2012. doi:10.1109/TIA.2011.2182329

[21] J. Klima, "Analytical Investigation of an Induction Motor Fed from Four-Switch VSI with a New Space Vector Modulation Strategy," IEEE Transactions on Power Electronics, vol. 21, no. 6, pp. 1618-1617, 2006. doi:10.1109/TEC.2005.858067

[22] B. El Badsi, B. Badii, A. Masmoudi, "DTC Scheme for a Four-Switch Inverter-Fed Induction Motor Emulating the Six-Switch Inverter Operation" IEEE Transactions on Power Electronics, vol. 28, no. 7, pp. 3528-3538, 2013. doi:10.1109/TPEL.2012.2225449

[23] D. Souvik, N. M. Shankar, K. S. Sanjib, K. P Sanjib, "Application of Four-Switch-Based Three-Phase Grid-Connected Inverter to Connect Renewable Energy Source to a Generalized Unbalanced Microgrid System," IEEE Transactions on Industrial Electronics,vol. 60, no. 3, pp. 1204-1215, 2013. doi:10.1109/TIE.2012.2202350

[24] S. Sajeev, M. Anna, "Novel Cost Effective Induction Motor Drive with Bridgeless PFC and Four Switch Inverter," International Conference on Emerging Trends in Communication Control Signal Processing and Computing Applications, 2013. doi:10.1109/C2SPCA.2013.6749436

[25] J. Klima, "Analytical Investigation of an Induction Motor Fed from Four-Switch VSI With a New Space Vector Modulation Strategy," IEEE Transactions on Power Electronics, vol. 21, no. 6, pp. 1618-1617, 2006. doi:10.1109/TEC.2005.858067

[26] M. N. Uddin, T. S. Radwan, M. A. Rahman, "Fuzzy-Logic-Controller-Based Cost-Effective Four-Switch Three-Phase Inverter-Fed IPM Synchronous Motor Drive System," IEEE Transactions on Power Electronics, vol. 42, no. 1, pp 21-30, 2006. doi:10.1109/TIA.2005.861277

[27] M. S. Zaky, M. K. Metwaly, "A Performance Investigation of a Four-Switch Three-Phase Inverter-Fed IM Drives at Low Speeds Using Fuzzy Logic and PI Controllers," IEEE Transactions on Power Electronics, vol. 32, issue, 5, 2017. doi:10.1109/TPEL.2016.2583660

[28] M. Narimani, G. Moschopoulos, "A New Single-Phase Single-Stage Three-Level Power Factor Correction AC–DC Converter," IEEE Transactions on Power Electronics, vol. 27, no. 6, pp. 2888- 2899, 2012. doi:10.1109/TPEL.2011.2174256

[29] R.-Emil Precup, S. Preitl, P. Korondi, "Fuzzy controllers with maximum sensitivity for servosystems," IEEE Transactions on Industrial Electronics, vol. 54, no. 3, pp. 1298-1310, 2007. doi:10.1109/TIE.2007.893053

[30] D. Martín, R. del Toro1, R. Haber, J. Dorronsoro, "Optimal tuning of a networked linear controller using a multi-objective genetic algorithm and its application to one complex electromechanical process," International Journal of Innovative Computing, Information and Control, vol. 5, no. 10 (B) pp. 3405-3414, 2009.

[31] T. Gabriel, I. Barbi, "Isolated three-phase high power factor rectifier based on the SEPIC converter operating in discontinuous conduction mode" IEEE Transactions on Power Electronics, vol. 28, no.11, pp 4962-4969, 2013. doi:10.1109/TPEL.2013.2247775

[32] G. Bhuvaneswari, B. Singh, S. Singh, "Three-phase single stage medium power supply using Cuk converter," Power Electronics (IICPE), 2012 IEEE 5th India International Conference on. IEEE, 2012. doi:10.1109/IICPE.2012.6450485